

University of Dundee

Thermal properties of lightweight concrete incorporating high contents of phase change materials

Sukontasukkul, Piti; Uthaichotirat, Pattra; Sangpet, Teerawat; Sisomphon, Kritsada; Newlands, Moray; Siripanichgorn, Anek

Published in:
Construction and Building Materials

DOI:
[10.1016/j.conbuildmat.2019.02.152](https://doi.org/10.1016/j.conbuildmat.2019.02.152)

Publication date:
2019

Document Version
Peer reviewed version

[Link to publication in Discovery Research Portal](#)

Citation for published version (APA):

Sukontasukkul, P., Uthaichotirat, P., Sangpet, T., Sisomphon, K., Newlands, M., Siripanichgorn, A., & Chindaprasirt, P. (2019). Thermal properties of lightweight concrete incorporating high contents of phase change materials. *Construction and Building Materials*, 207, 431-439. <https://doi.org/10.1016/j.conbuildmat.2019.02.152>

General rights

Copyright and moral rights for the publications made accessible in Discovery Research Portal are retained by the authors and/or other copyright owners and it is a condition of accessing publications that users recognise and abide by the legal requirements associated with these rights.

- Users may download and print one copy of any publication from Discovery Research Portal for the purpose of private study or research.
- You may not further distribute the material or use it for any profit-making activity or commercial gain.
- You may freely distribute the URL identifying the publication in the public portal.

Take down policy

If you believe that this document breaches copyright please contact us providing details, and we will remove access to the work immediately and investigate your claim.

1 Thermal Properties of Lightweight Concrete Incorporating High Contents of Phase Change

2 Materials

3 Piti Sukontasukkul¹, Pattrra Uthaichotirat¹, Teerawat Sangpet², Kritsada Sisomphon³, Moray
4 Newlands⁴, Anek Siripanichgorn⁵, Prinya Chindapasirt⁶

5 ¹Construction and Building Materials Research Center, Department of Civil Engineering, King
6 Mongkut's University of Technology North Bangkok

7 ²Department of Mechanical and Aerospace Engineering, King Mongkut's University of
8 Technology North Bangkok, Bangkok, Thailand

9 ³Siam Research and Innovation Co., Ltd., Saraburi, Thailand

10 ⁴School of Science and Engineering, University of Dundee, UK

11 ⁵Department of Civil Engineering, King Mongkut University of Technology Thonburi

12 ⁶Sustainable Infrastructure Research and Development Center, Department of Civil
13 Engineering, Khon Kaen University, Thailand.

14 Abstract

15 This research investigated the latent heat and energy storage of lightweight concrete
16 containing high contents of phase change material (PCM) (up to about 7.8% by weight of
17 concrete). PCM - Polyethylene Glycol (PEG) with a fusion temperature of approximately 42-
18 46°C was impregnated into porous lightweight aggregates up to 24% by weight. The PCM
19 aggregates were then used to replace normal lightweight aggregate at a rate of 0, 25, 50, 75
20 and 100% by volume. The samples were subjected to series of experiments such as
21 compressive strength (EN12390-3 2002), flexural strength (ASTM C78), thermal conductivity

22 (ASTM C518) and the thermal storage of phase change materials examined using a heat flow
23 meter apparatus (ASTM C1784) at the age of 28 days. Results show that the existence of PCM
24 aggregates affects both mechanical and thermal properties of concrete to different degrees.
25 The mechanical properties appear to improve with increasing PCM aggregate content. For
26 thermal properties such as thermal conductivity and specific heat, the state of the PCM (liquid
27 or solid state) as well as the testing temperature during the test, show significant influence
28 on the obtained results. The latent heat was found to increase proportionally with the
29 increasing PCM aggregate replacement rate.

30 **Keywords:** Latent Heat, Heat Storage, Specific Heat, Thermal Conductivity, Lightweight
31 Aggregate, Lightweight Concrete, Phase Change Material, PCM carrier.

32 **1. Introduction**

33 Global energy demand is increasing and is expected to continue to increase every year. From
34 1980 to 2012, the energy consumption of three of the world's largest economies (USA, China
35 and the EU) increased by 85%. Interestingly, the energy demand from the building sector has
36 been reportedly increasing at a greater rate than the commercial sector [1]. In 2010, global
37 energy demand in the building sector was approximately 115 EJ, 32% of total global energy
38 demand [2]. In Thailand, energy usage in the household sector accounts for about 24% of
39 total energy production [3]. Most of it is spent on conditioning the temperature in houses and
40 buildings because Thailand is located in a hot and humid climate region. In order to reduce
41 the energy consumption, construction materials with good thermal insulation are necessary.
42 Conventionally, thermal properties of concrete can be enhanced by simply incorporating air
43 voids into concrete mixture by means of utilizing porous aggregates or by using aerated
44 cement paste. Although the existence of air voids in concrete enhances the thermal

45 insulation, it also interferes with the mechanical properties. It is expected that 5% of
46 compressive strength drops for every 1% of air volume inserted into concrete.

47 To enhance thermal performance with the least effect on existing properties, thermal
48 enhancing agents such as phase change materials (PCM) can be used. PCMs are high latent
49 heat materials capable of changing phase at a specific temperatures. This allows materials to
50 improve thermal storage capabilities through latent heat captivity. The PCM begins to melt
51 as the temperature approaches the melting point, and a large amount of latent heat is
52 absorbed at near constant temperature until it is fully melted. On the contrary, as the
53 temperature cools down to reach the solidification point, liquid PCM begins to solidify and
54 the stored latent heat is released back to the environment. This ability can be used to enhance
55 heat storage, slow down rate of heat transmission, and shift the period of peak temperature
56 [4-8].

57 The application of PCM in house components began in 1947 when Glauber's salts in steel
58 drums were used as heat storage components in Dover, Massachusetts [9]. Trombe walls are
59 another example of an early PCM applications. Invented by Felix Trombe, a French engineer,
60 they are passive solar walls constructed from masonry bricks with a void containing water in
61 the middle. The water provided heat storage capacity during the day time and released out
62 during the night time.

63 The use of PCMs in construction materials has developed over time. Oliver [10] studied
64 thermal behavior of gypsum boards containing 45% by weight of PCM. The results showed
65 that gypsum boards (15 mm thick) with PCM can store energy up to 5 times of conventional
66 laminated gypsum boards within temperature ranges of 20-30°C. Silva, et al. [11] worked with
67 incorporation of PCM macro encapsulated into typical Portuguese clay brick masonry
68 enclosure walls and subjected them to series of temperature ranges in a climate chamber.

69 The results showed that the walls with PCM can reduce the indoor temperature swing from
70 10°C to 5°C and delay the duration to reach peak temperature up to about 3 hours.

71 In the case of cementitious materials, there are number of ways to incorporate PCM into
72 concrete. The simplest one is to treat PCM as a constituent material to be mixed with
73 concrete. Cunha et al [12] reported the increase in workability and the reduction in absorption
74 when PCM is added into concrete mixture. Sukontasukkul et al [13] tested thermal
75 performance of exterior wall panels plastered with mortars mixed with PCM (polyethylene
76 glycol type, PEG). The PEG mortar exhibited better workability and water retention. The pull-
77 out and compressive strength also increased with the increasing PCM content. The exterior
78 walls plastered with PCM mortar exhibited better thermal storage and extending the time to
79 reach peak temperature. However, after a number of temperature cycles, leaking of melted
80 PCM was regularly observed.

81 An effective way in preventing PCM leakage is using encapsulation techniques [14-16]. By
82 adopting encapsulation, the PCM is stored inside small polymeric spherical capsules. The
83 method not only prevents leakage, but also provides a large surface area of heat transfer.
84 However, due to the increase in porosity and weak bond strength, an evident drop in strength
85 is regularly observed. With this disadvantage, the use of PCM encapsulation is limited to a
86 very small fractions (less than 10%). Cao et al [17] determined the thermal properties of
87 concrete mixed with microencapsulated PCM (MPCM) from 0 to 2.7% by weight of concrete.
88 They reported no change in the value of specific heat due to the low MPCM concentrations.
89 The latent heat was found to increase linearly from 0 to 2.25 J/g as the MPCM content
90 increased from 0 to 2.7% by weight. The compressive strength, on the other hand, was found
91 to decrease significantly (up to 51%) due to high porosity and poor bond. Sakulich et al [18]
92 used fine aggregate impregnated with PCM to reduce freeze/thaw damage of bridge deck

93 concrete. They recommended a PCM dosage of 50 kg/m³ of PCM to increase bridge deck
 94 service life by at least one year.

95 In this study, in order to increase the PCM concentrations, the use of porous aggregates as a
 96 PCM carrier was proposed. The PCM aggregates were prepared by impregnating PCM
 97 (polyethylene glycol type, PEG) into aggregates at elevated temperatures. During the
 98 specimen preparation, the PCM aggregates were then used to replace the regular porous
 99 aggregates at the rate of 25 %, 50 %, 75 % and 100% by volume which equals to about 2.1 %,
 100 4.0 %, 6.0 % and 7.8% by weight of concrete, respectively. The specimens were subjected to
 101 a series of tests including density, absorption, compressive and flexural strength, thermal
 102 conductivity and thermal storage properties (specific heat, sensible and latent heat). The
 103 effect of PCM content on thermal conductivity and thermal storage properties such as specific
 104 heat, total, sensible and latent heat were also investigated. In addition, the effect of PCM
 105 state on the thermal conductivity tests was also examined.


106 2. Experimental Procedure

107 2.1 Materials

- 108 • Portland Cement Type I (ASTM C150) with specific gravity of 3.15.
- 109 • River sand passing sieve no. 4 with FM = 2.45. and specific gravity of 2.47.
- 110 • Lightweight aggregates with properties given in Table 1.
- 111 • Phase change material: Polyethylene glycol type 1450 with properties as shown
 112 in Table 2.

113 **Table 1** Properties of lightweight aggregates

Specification	Value	
Maximum particle size	10 mm	

Unit weight	732 kg/m ³	
Percent of voids	72	
Bulk specific gravity (Dry Basis)	1.08	
Bulk specific gravity (SSD Basis)	1.25	
Apparent specific gravity	1.3	
Apparent porosity	18.1%	
Percent absorption	17.5%	

114

115 **Table 2** Properties of Polyethylene Glycol type 1450

Specification	Unit	Test Result
Melting point	°C	42-46
Specific gravity	at 25 °C	1.09
Latent heat	kJ/kg	155
Thermal conductivity*	W/m K.	0.23
Liquid specific heat*	J/kg.K	2100
Flash point	°C	285
Range of Avg. Molecular Weight		1305-1595
Physical Form		Flake

116

117 **2.2 Preparation of PCM aggregates**

118 The polyethylene glycol (PEG) was impregnated into lightweight aggregates at two different
119 temperatures of 100 °C and 120°C. The process began with drying lightweight aggregates
120 using an oven at 100°C for 24 hours. After that the aggregates were placed in containers and
121 submerging with melted PCM. The containers were placed in the oven at two different

122 degrees: 100 °C and 120 °C for up to 8 hours. Every hour, samples were extracted and weighed
 123 to measure weight change and calculate the degree of impregnation using equation 1.

$$124 \quad \%Impregnation = \frac{W_t - W_i}{W_i} \times 100 \quad (1)$$

125 where W_i is the initial dry weight before submersion.

126 W_t is the weight after submerging in PCM at any time.

127

128 The process continued until the highest impregnation percentage is reached and weight
 129 change becomes constant over time. The time to reach the highest percentage was used in
 130 preparing the PCM lightweight aggregates (PCM-LWA).

131 2.3 Preparing concrete samples

132 The PCM lightweight aggregates (PCM-LWA) were prepared using the results obtained from
 133 Section 2.2 for the highest impregnation level at the shortest time. The mix proportions by
 134 weight for the control mix were set at 1 : 0.42 : 1.02 : 1.15 (Cement : Water : LW aggregate :
 135 Sand). Conventional lightweight aggregate (LWA) was replaced by PCM-LWA at a rate of 25 %
 136 to 100% by volume with the PCM weight being equivalent to 2.1 to 7.8%. Detailed mix
 137 proportions are given in Table 3.

138 **Table 3** Mix proportions for 1 m³

Type of Concrete*	Unit weight kg/m ³					Equivalent PCM Content
	LWA	PCM-LWA	Sand	Cement	Water	(% by weight of concrete)
100LOP	488	0	550	477	200	0.0

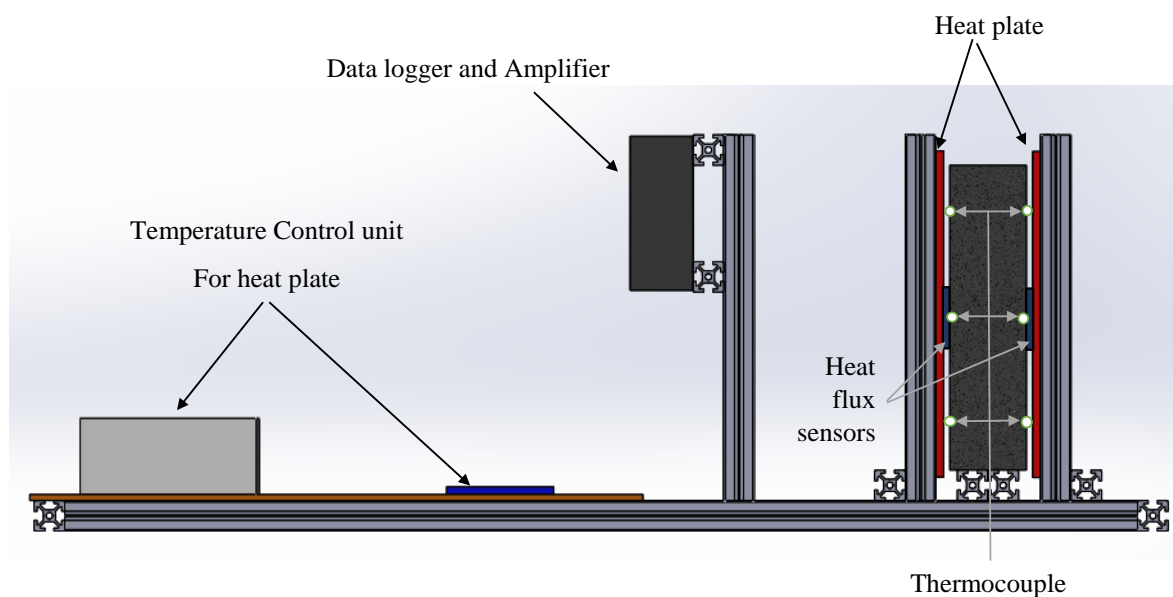
75L25P	366	149	550	477	200	2.1
50L50P	244	298	550	477	200	4.0
25L75P	122	447	550	477	200	6.0
0L100P	0	595	550	477	200	7.8

139 *Note: aLbP a = volume fraction of LWA and b = volume fraction of PMC-LWA

140 2.4 Experimental series

141 After the specimens were prepared and cured for 28 days, they were subjected to a series
142 of experiments as follows:

- 143 • Density test (ASTM C138)
- 144 • Water absorption test (ASTM C642)
- 145 • Compressive strength (EN12390-3 2002)
- 146 • Flexural strength (ASTM C78)
- 147 • Steady-state thermal transmission properties by means of heat flow meter
148 apparatus (ASTM C518-17)
- 149 • Thermal storage properties of phase change materials and products (ASTM C1784
150 – 14)



151

152

Fig. 1 Heat flow meter apparatus

153 **Table 4** Specification of the measurement

Heat Plate	Temperature of 30 °C – 100 °C
Thermocouple wire	Type K, -50 °C to 250 °C
Heat flux sensor (Hioki)	
Temperature range	Sensor: -40 °C to 150 °C, Cords: -40 °C to 120 °C
Heat flow	769 w/m ² - 384,615 w/m ²
Data logger (Hioki LR8431-20)	
Parameters	Voltage, heat flow, thermocouple, pulse, RPM
Heat flow and Voltage	±10 mV to ±60 V, 1-5V, Max. resolution 500 nV
Temperature range	-200 °C to 1800 °C (Depend on type of thermocouple)
Type of thermocouples	K, J, E, T, N, R, S, B
Recording period	10 ms – 1 hour
Display	Graph and Raw data

154

155 **2.5 Thermal Test and Data Analysis**

156 The thermal tests were carried out using a heat flow meter apparatus (Fig.1). The apparatus
157 was capable of measuring energy storage in the test specimen, which in turn was used in
158 determining thermal conductivity, specific heat, and latent heat of PCM products. The
159 apparatus consisted of two hot plate exchangers connected to a control unit. A specimen with
160 dimension of 200 x 200 x 50 mm was placed between the two hot plates. Two heat flux
161 sensors and eight K-type thermocouples were installed on both surfaces and in the middle of
162 the sample to measure temperature variations and heat fluxes throughout the sample. To
163 minimize the heat transferred to the surrounding environment, a 50 mm thick of insulating
164 wool was used to cover around lateral sides of the sample. The heat transfer through the
165 concrete sample is assumed to be one dimensional condition. All sensors and thermocouples
166 were connected to an automatic data acquisition box. The apparatus specification is given in
167 Table 4.

168

169 **2.5.1 Thermal conductivity**

170 In this study, the thermal conductivities of concrete mixed with PCM-LWA were measured at
171 two temperatures above and below the melting point of PCM (25 and 55°C) to investigate the
172 effect of PCM state (solid and liquid) on the thermal conductivity.

173 To begin the test, both heat plates were kept at a constant temperature until the heat flux is
174 constant and the temperature of the sample is the same as the heat plates. Then the
175 temperature of one of the heat plates was set to a new target temperature. The temperature
176 difference causes the heat to transfer through the concrete sample. The heat flux sensor
177 measured the total heat required for the sample to reach equilibrium (steady-state). At the

178 steady-state, the test was terminated. The recorded data was used to calculate the thermal
179 conductivity by:

$$180 \quad \lambda_T = S \cdot E \cdot \left(\frac{L}{\Delta T} \right) \quad (1)$$

181 where λ_T is thermal conductivity at any temperature ($\text{W}/\text{m} \cdot \text{K}$), S is the calibration factor of
182 the heat flux transducer ($\text{W}/\text{m}^2/\text{V}$), E is heat flux transducer output (V), L is the distance
183 between the heat plates (m) and ΔT is temperature difference across the specimen (K).

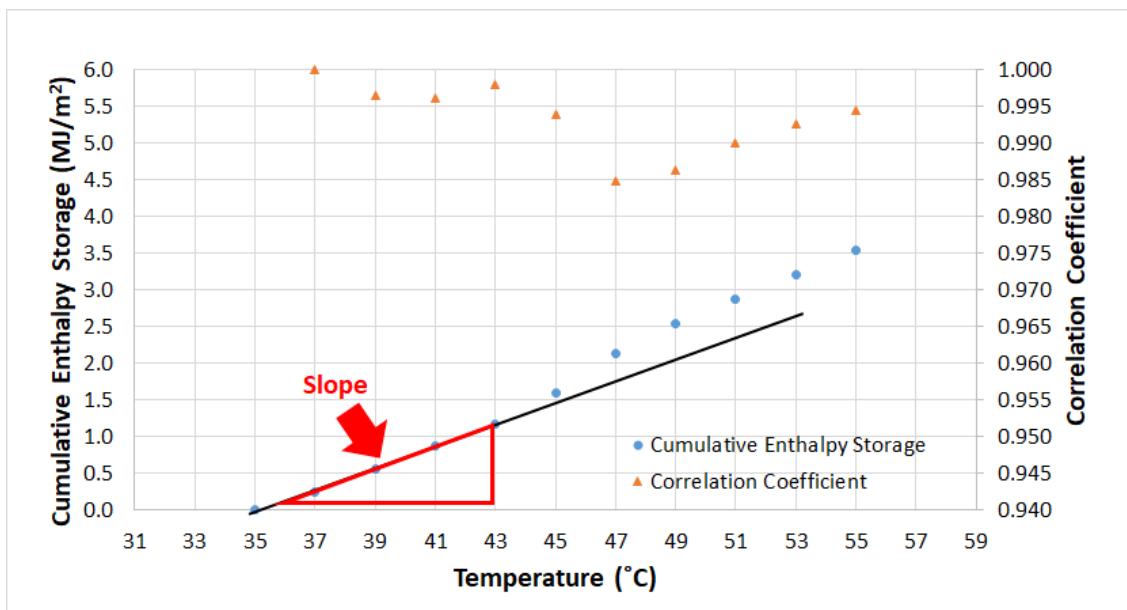
184 **2.5.2 Latent heat**

185 To test for latent heat, the energy storage in a specimen over a temperature range was
186 determined. At the beginning of the test, the temperatures of both heat plates were
187 increased from room temperature to the beginning temperature (35°C). The heat flow was
188 measured simultaneously until the heat plates and specimen reached the same temperature
189 level and entered steady-state. The steady-state was defined as the reduction in the amount
190 of energy entering the specimen from both plates to a very small and near constant value
191 (ASTM C1784). The total energy was measured and recorded. Next, the two heat plates were
192 set to the new identical temperature and held until the steady state was achieved again. The
193 energy absorbed by the specimen was also recorded. Repeating the similar procedure until
194 the steady state of the final temperature was achieved, the test was then terminated. Using
195 the series of temperature step change, the enthalpy and accumulated enthalpy storage were
196 determined and used in calculating the specific, sensible and latent heats.

197 In this study, since the melting temperature the PCM was around $42\text{-}46^\circ\text{C}$, the range of test
198 temperature was set at 35°C to 55°C with 2°C incrementing steps to cover PCM at both solid
199 and liquid states. First, the graph between the cumulative enthalpy storage versus time was

200 plotted and used to determine two specific heats: the specific heat of a solid PCM product,
 201 C_{pS} (below melting point) and the specific heat of a melted PCM product, C_{pM} (above melting
 202 point). Both specific heats are calculated using the baseline of the correlation graph between
 203 the accumulate enthalpy and temperature at each step. The baseline is obtained by
 204 performing a linear regression using the first data and subsequent data points until the
 205 regression coefficient (R^2) is smaller than 0.995. The slope of the line connecting the first to
 206 the last data point with R^2 greater than 0.995 is defined as the specific heat values (Fig.2). This
 207 procedure was performed under both solid and liquid conditions to obtained C_{pS} and C_{pM} ,
 208 respectively.

209



210

211 **Fig. 2** Determination of Specific Heat using Baseline Correlation

212 To calculate the latent heat, it was assumed that the total enthalpy stored in the specimen at
 213 the PCM active range consists of 2 parts: sensible and latent heats. The total heat (h_t) is the
 214 summation of enthalpy over the PCM active temperature range using Eq.1.

215
$$h_t = \sum_{T_L}^{T_U} \Delta h \quad (1)$$

216 The sensible heat (h_s) was determined using the specific heats below and above the active
 217 range of the PCM (i.e., C_{pS} and C_{pM}) equals to:

$$218 \quad h_s = \frac{(C_{pS} + C_{pM})(T_U - T_L)}{2} \quad (2)$$

219 The latent heat of specimen with PCM product equals to the difference between the total
 220 heat and the sensible heat.

$$221 \quad h_l = h_t - h_s = \sum_{T_L}^{T_U} (\Delta h) - \frac{(C_{pS} + C_{pM})(T_U - T_L)}{2} \quad (3)$$

222 where h_l is the latent heat of PCM product, h is the enthalpy (J/m^2), T_U is an upper temperature
 223 limit of the PCM active Range ($^{\circ}C$), T_L is a lower temperature limit of the PCM active Range
 224 ($^{\circ}C$), C_{pS} is the specific heat of a solid PCM product and C_{pM} is the specific heat of a melted
 225 PCM product.

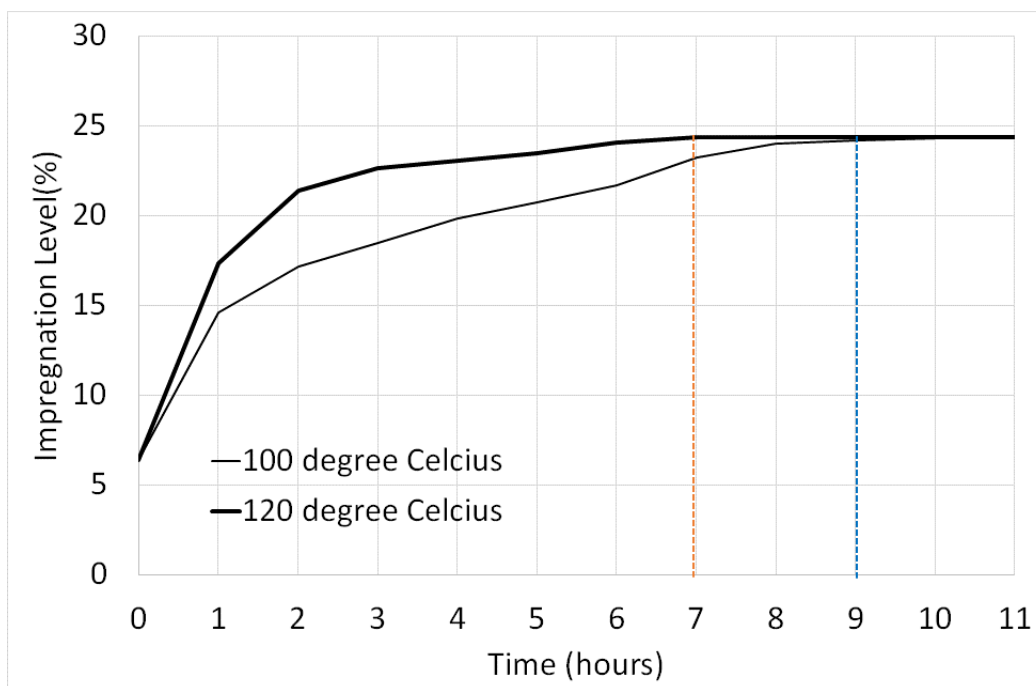
226

227 **3. Results and discussion**

228 **3.1 PCM Impregnation**

229 The PCM was impregnated into the lightweight aggregates using the method described in
 230 Section 2.2. The relationship between weight change and time is shown in Fig. 3. As soon as
 231 the lightweight aggregates are submersed into the melted PCM, the weight increases
 232 immediately by approximately 7% due to self-sorptivity of the aggregates. After that the
 233 weight increases gradually with time until reaching the steady state. At the steady state, the
 234 maximum impregnation level of 24% by weight is achieved. The temperature level plays an
 235 important role on the time taken to reach the steady state. The time to steady state decreases
 236 with the increasing temperature, with steady state of aggregates impregnated under $120^{\circ}C$
 237 achieved within 7 hours compared to 9 hours for those at $100^{\circ}C$. The shorter duration is partly
 238 due to a decrease in viscosity of the PEG with increasing temperature. Fig. 4 shows the

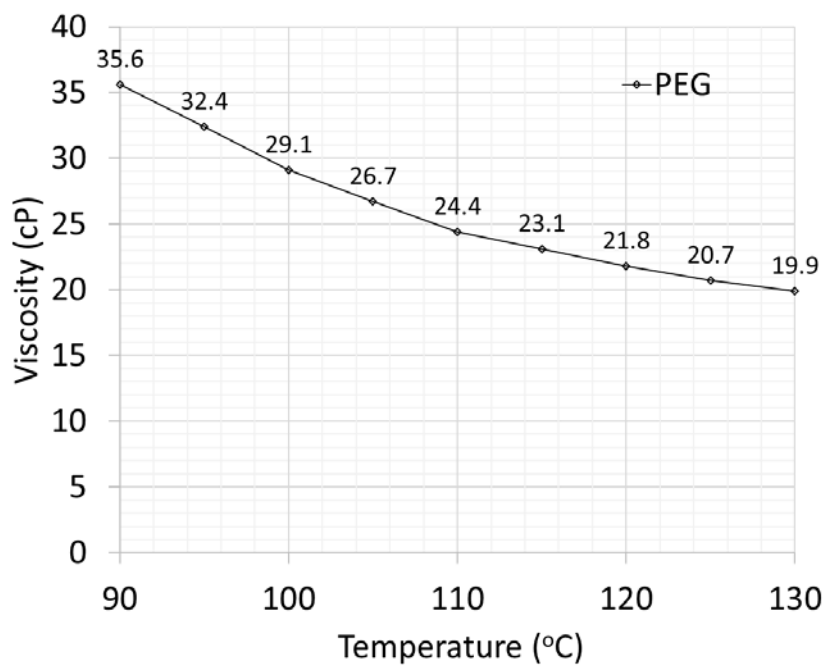
239 decrease in viscosity from 29.1 cP to 21.8 cP as the temperature increases from 100 °C to
 240 120 °C, respectively.



241

242

Fig. 3 Change in impregnation level with time



243

244

Fig. 4 Change in viscosity of PEG with Temperature

245 **3.2 Properties of PCM-LWA**

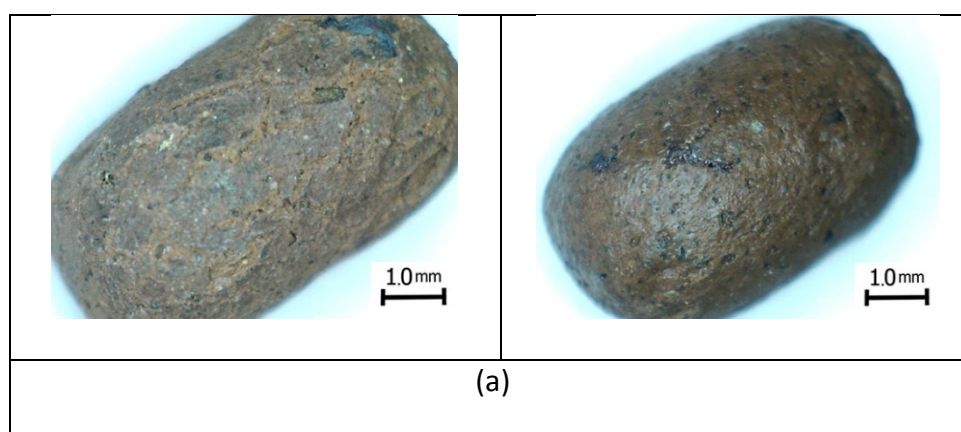
246 PCM-LWA samples exhibit lower absorption and higher specific gravity than LWA without
 247 PCM (Table 5). This is due to the effect of PCM filling pores inside the aggregates. Figure 5
 248 shows a comparison between PCM-LWA and LWA on the external surfaces and cut sections.
 249 The surface of PCM-LWA appears to be less porous than LWA with evidence of PCM coating
 250 the outer surface. The 100x images of the cut sections also show the effect of PCM filling up
 251 pore spaces in the PCM-LWA.

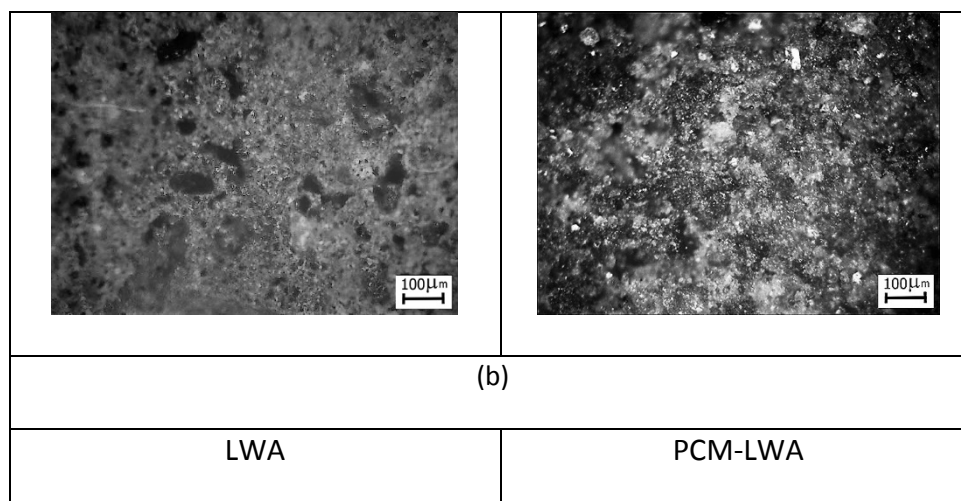
252

253 **Table 5** Properties of LWA and PCM-LWA

	Unit	LWA	PCM-LWA	Difference (%)
Percent absorption	%	16.0	0.17	- 98.9 ²⁵⁵
Specific gravity		1.0	1.30	+ 22.0 ²⁵⁶ 257

258





259

260 **Fig. 5** Comparison between (a) Surface and (b) Cut section of PCM-LWA and LWA.

261

262 3.3 Properties of Concrete mixed with PCM-LWA

263 3.3.1 Density and Absorption

264 The replacement of LWA with PCM-LWA in concrete increases the density and lowers the
 265 absorption of concrete. This is because the PCM-LWA is denser than LWA and by gradually
 266 increasing the ratio of PCM-LWA, the concrete density increases and the absorption
 267 decreases. Figure 6 shows the increase in density from 1747 kg/m³ to 1903 kg/m³ as the LWA
 268 is replaced by the PCM-LWA up to 100% by volume. The absorption also decreases 2.20 % to
 269 1.75 % when the LWA is entirely replaced by the PCM-LWA. The replacement of porous
 270 aggregates with denser aggregates (PCM-LWA) is a key role in the increasing density and
 271 decreasing absorption.

272

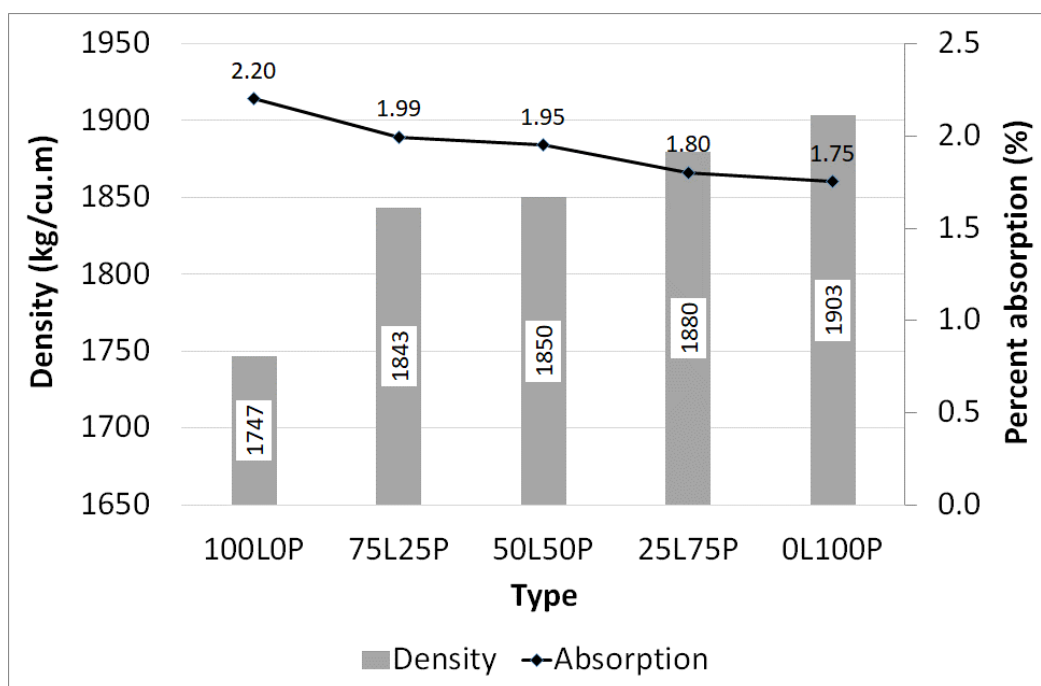
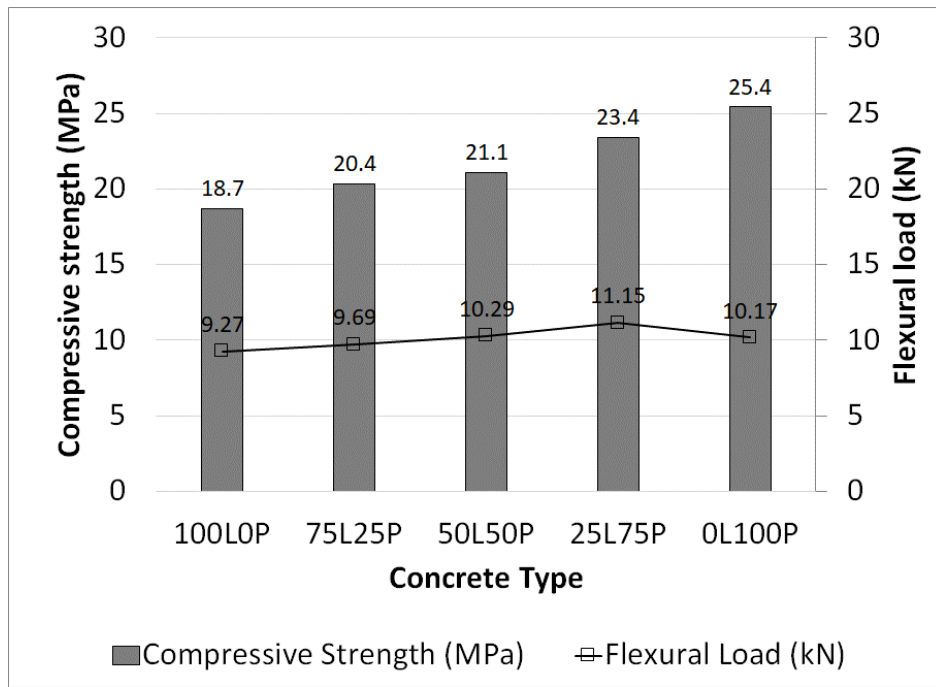


Fig. 6 Density and Absorption of Concrete mixed with PCM-LWA

3.3.2 Compressive and Flexural strength of concrete

Results of the compressive and flexural strengths are presented in Fig. 7. The results show that increasing the ratio of PCM-LWA causes an increase in compressive strength of concrete. The maximum compressive strength of 25.42 MPa is obtained at 100% replacement rate. The increase in compressive strength is partly due to improvement of PCM-LWA properties which is higher in density and less porous.

In the case of flexural load, the load capacity increases with the increasing PCM-LWA replacement ratio up to 75% then decreased. This rate is defined as the optimum replacement ratio for bending load where the maximum load of 11.15 kN is obtained. The small reduction in flexural load capacity is due to effect of PCM coating around the surface of lightweight aggregate which could negatively affect the bond between aggregates and cement paste. The effect of PCM coating is more pronounced under flexural load due to the nature of flexural load which creates tensile stresses at the lower half of the specimen and these tensile stresses are sensitive to the aggregate-paste bond strength.

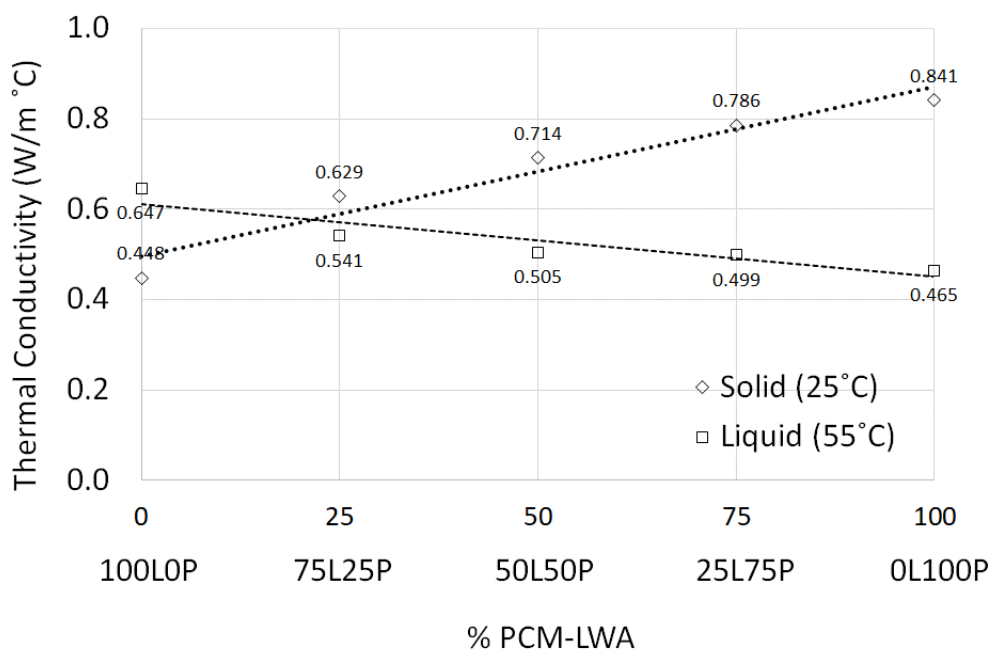


289

290 Fig. 7 28 Day-Compressive strength and flexural load of concrete mixed with PCM-LWA

291 **3.3.3 Thermal conductivity**

292 In this study, the thermal conductivity (TC) was measured at temperature levels below and
 293 above the PCM melting temperature (42 °C - 46°C) to investigate the effect of PCM state on
 294 TC. Two temperatures were selected: 25 °C and 55 °C. The testing procedure as described in
 295 Section 2.5.1 was carried out and the results are plotted in Fig. 8.



296

297 Fig. 8 Thermal Conductivity of PCM-LWA Concrete under Solid and Liquid State

298 When tested with PCM under solid condition or at 25°C, the thermal conductivity of concrete
 299 with conventional LWA (without PCM) was 0.448 W/m°C. With PCM-LWA, the TC with PCM
 300 under solid state (TC_s or TC_{25}) increased with the increasing PCM-LWA content. The highest
 301 TC_s of 0.841 W/m°C was observed in concrete with 100% PCM-LWA (0L100P). The increase in
 302 thermal conductivity is mainly due to the increasing solid content of concrete. Since the solid
 303 PCM is replacing pores inside the aggregates, it reduces the air content and causes the TC to
 304 increase.

305 Contrarily, when tested with PCM under liquid state or temperatures higher than the melting
 306 point of PCM (55°C), the thermal conductivity at 55°C (TC_{55}) of the concrete with conventional
 307 LWA is observed at 0.647 W/m°C which is about 30% higher than specimens tested at 25°C.
 308 This shows that the TC is directly influenced by the level of testing temperature. The TC was
 309 found to decrease with the increasing PCM-LWA content. This is mainly due to the effect of
 310 PCM phase changing process and energy storage phenomenon. When the temperature rises

311 to around the melting temperature, the PCM begins to melt and store energy. The PCM
 312 cannot be considered as regular liquid because it has an ability to store heat in form of latent
 313 heat during phase transition and this ability plays an important role on the decreasing the TC.
 314 It causes the temperature to remain constant until all PCM changes into liquid state, the rate
 315 of heat transfer slows down, lowering the thermal conductivity. Similar finds are also reported
 316 by Cao et al [17]. In their study, the thermal conductivity of concrete with melted PCM in
 317 microencapsulate form was found to reduce by 38% (from about 1.25 to 0.9 W/m°C) when
 318 the PCM concentration increased from 0 to 2.7 % by weight of concrete.

319 The relationship between the PCM-LWA replacement percentage and thermal conductivity
 320 can be expressed by equation 3 and equation 4 below.

321 Thermal Conductivity under solid state:

$$322 \quad TC_{25} = 0.0038(\%A_{PCM}) + 0.495 \quad (3)$$

323 Thermal Conductivity under liquid state:

$$324 \quad TC_{55} = -0.0016(\%A_{PCM}) + 0.6126 \quad (4)$$

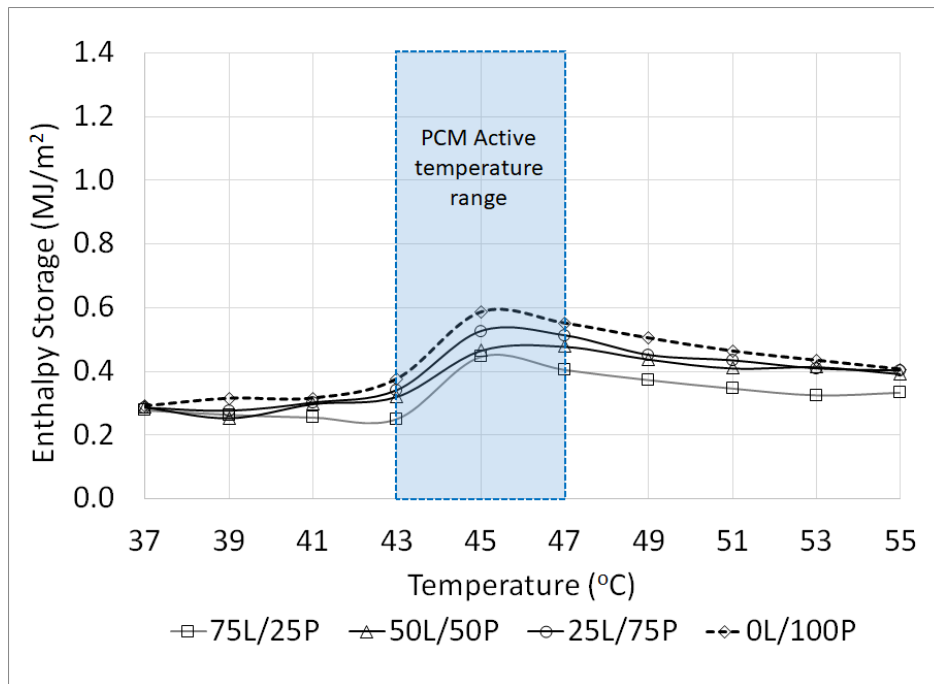
325 where TC_{25} is the thermal conductivity measured under at 25°C (solid PCM), TC_{55} is the
 326 thermal conductivity measure at temperature of 55°C (melted PCM), $\%A_{PCM}$ is the
 327 replacement percentage of PCM-LWA over the LWA.

328 **3.3.4 Enthalpy storage**

329 The enthalpy storage of concrete mixed with PCM aggregates is plotted in Fig. 9. At the
 330 temperature below the PCM melting point, the enthalpy storages of all concretes are in
 331 similar range within a narrow gap between 0.260 MJ/m² to 0.315 MJ/m² (at 41°C). The total
 332 heat storage in this range of temperature is the direct result of the sensible heat.

333 Within the PCM active range (42 °C to 46 °C), the enthalpy storage increases for all specimen
334 types due to the effect of energy storage in the PCM during the phase changing process (latent
335 heat). The maximum enthalpy is reached at a temperature of 45°C. The enthalpy storage is
336 found to increase from 57 % to 86% depending on the PCM aggregate content. The total heat
337 at this range is assumed to be consisting of two parts: latent heat and sensible heat.

338 At temperatures higher than 45°C, the enthalpy storage begins to decrease slowly with
339 increasing temperature. This shows that most of the PCM is melted at 45°C and the effect of
340 latent heat begins to cease after this although to varying degrees. The enthalpy storage of the
341 concrete with higher PCM aggregate contents appears to decrease at slower rate than those
342 with lower PCM aggregate content. This phenomenon indicates that the PCM remains active
343 even beyond the perceived PCM active range. The enthalpy storage approaches near constant
344 values at different temperatures depending the PCM aggregate content (51 °C, 51 °C, 53 °C
345 and 55°C for 75L/25P, 50L/50P, 25L/75P and 0L/100P, respectively). At temperatures of 55°C,
346 when the enthalpy storage of all concrete types drop to the narrow level between
347 0.333 MJ/m² to 0.406 MJ/m², it is believed that there is no latent heat effect remaining.
348 However, it must be noted that the enthalpy storage of concretes with melted PCM is
349 essentially higher than those with solid PCM by a range of 30 % to 38%



350

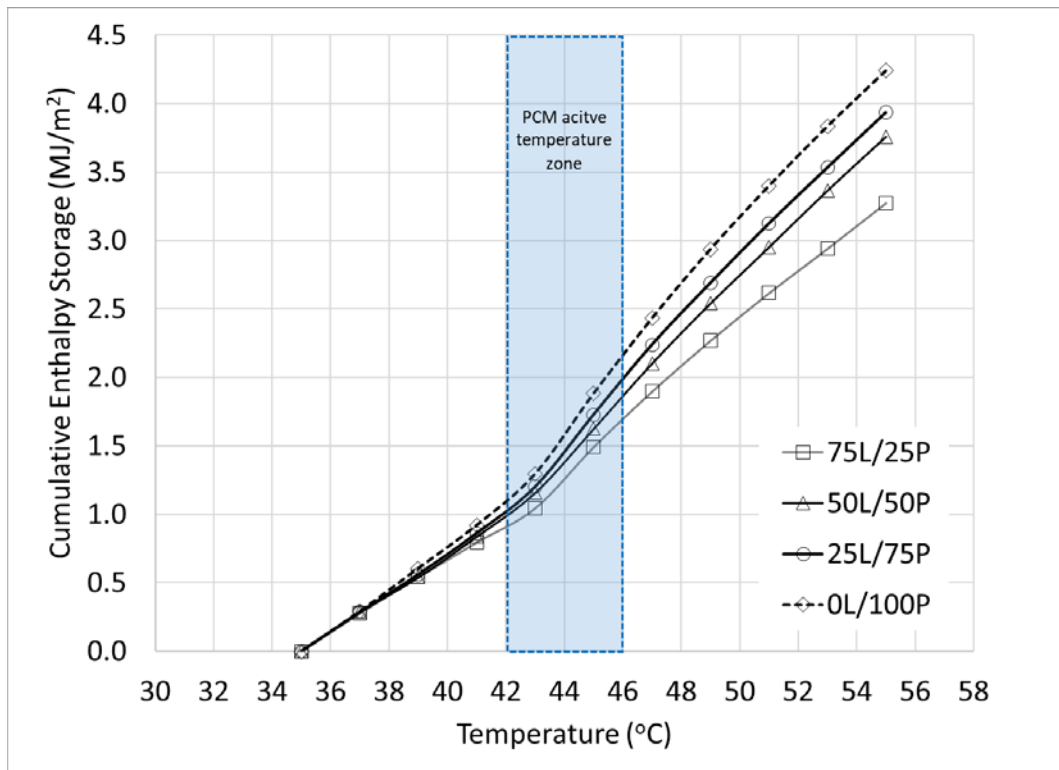
351

Fig. 9 Enthalpy Storage vs. Temperature

352 3.3.5 Specific heat

353 The specific heat is the amount of heat per unit mass required to raise the temperature of
 354 material by 1 °C. The specific heat can be calculated from the plot between accumulated
 355 enthalpy storage and temperature using the method described in Section 2.5.2. Test results
 356 are given in Table 6 and plotted in Fig. 10. According to the results, the specific heat of
 357 concretes with solid PCM (C_{ps}) are almost identical for all concrete types. The increasing PCM
 358 aggregate content from 25 % to 100% causes about 10% variation in specific heat (from 0.136
 359 to 0.150 (MJ/m²)/°C) which is considered low as compared to the PCM under liquid stage.

360 The specific heat is found to be higher under liquid state for all concrete types. Comparing at
 361 the same PCM aggregates content, C_{pM} is higher than C_{ps} by a range of 24 % to 55% for various
 362 concretes. Similar to the C_{ps} , the C_{pM} also increases with the PCM aggregate content. The
 363 increase of PCM aggregate from 25 % to 100% yields a 28% increase of the C_{pM} (from 0.168
 364 to 0.214 (MJ/m²)/°C).



365

366

Fig. 10 Cumulative enthalpy storage vs. Temperature

367 3.3.6 Latent heat

368 The results on latent heat along with the total heat and sensible heat storages during the PCM
 369 active range are given in Table 6. All of them are clearly affected by the PCM aggregate
 370 content by varying degrees. For the sensible heat, the increase of about 20% is observed.
 371 Since the sensible heat is strongly related to the specific heat (both C_{pS} and C_{pM}), the increase
 372 in specific heat due to PCM, especially in the C_{pM} , provides some impact on the sensible heat
 373 storage.

374 The latent heat storage, on the other hand, is the thermal property that is influenced by the
 375 PCM content. Therefore, the latent heat storage is expected to rise with the increasing
 376 amount of PCM aggregates. In this study, the peak latent heat (7,722 J/kg) is observed in
 377 0L100P (PCM content of 7.8%). With the PCM aggregate replacement increasing from 25 %

378 to 100%, an increase of the latent heat by 64% (from 0.447 MJ/m² to 0.635 MJ/m²) is
379 observed. The increase of latent heat with respected to PCM aggregate content clearly
380 demonstrated the possibility of incorporating high contents of PCM into concrete without
381 compromising other properties.

382 Although the latent heat capacity of concrete at 7.722 kJ/kg seems high when compared to
383 ordinary concrete, it still looks relatively small when compared to the latent capacity of pure
384 PCM at about 150 kJ/kg. This can be explained as follows. The amount of PCM used in the
385 concrete is approximately about 8% of the concrete weight. Therefore, the latent heat
386 obtained is less when compared to pure PCM. In addition, the unit weight of PCM concrete is
387 higher than PCM itself, when dividing the latent heat storage by weight of concrete, it gives
388 less latent heat per unit weight. The reported results are in line with work by Jayalath et al
389 [20]. In their study, the PCM with latent heat capacity of about 100 kJ/kg in encapsulated form
390 was mixed with cement mortar up to 55% by weight. They observed the latent heat capacity
391 ranged from 0.546 kJ/kg to 4.724 kJ/kg which is also small compared to the latent heat of the
392 PCM. Ramakrishnan et al [21] also conducted thermal tests on PCM impregnated into
393 expanded perlite aggregates. They found the latent heat capacity of the concrete mixed with
394 PCM aggregates varied from 35 J/g to 61 J/g depending on the surface coating condition as
395 compared to PCM of 133 J/g.

396 For total heat storage, an increase of 35% from 1.36 MJ/m² to 1.83 MJ/m² with increasing
397 PCM aggregate content was observed. Since the total heat storage is the summation of latent
398 heat and sensible storage, the increase of both contribute to the increase in total heat
399 storage.

400 Based on the results, linear relationships between the PCM aggregate replacement
 401 percentage and heat storage can be expressed by Equations 5, 6 and 7 (Fig.11).

$$402 \quad h_t = 0.62(\%A_{PCM}) + 1.22 \quad (5)$$

$$403 \quad h_s = 0.23(A_{PCM}) + 0.88 \quad (6)$$

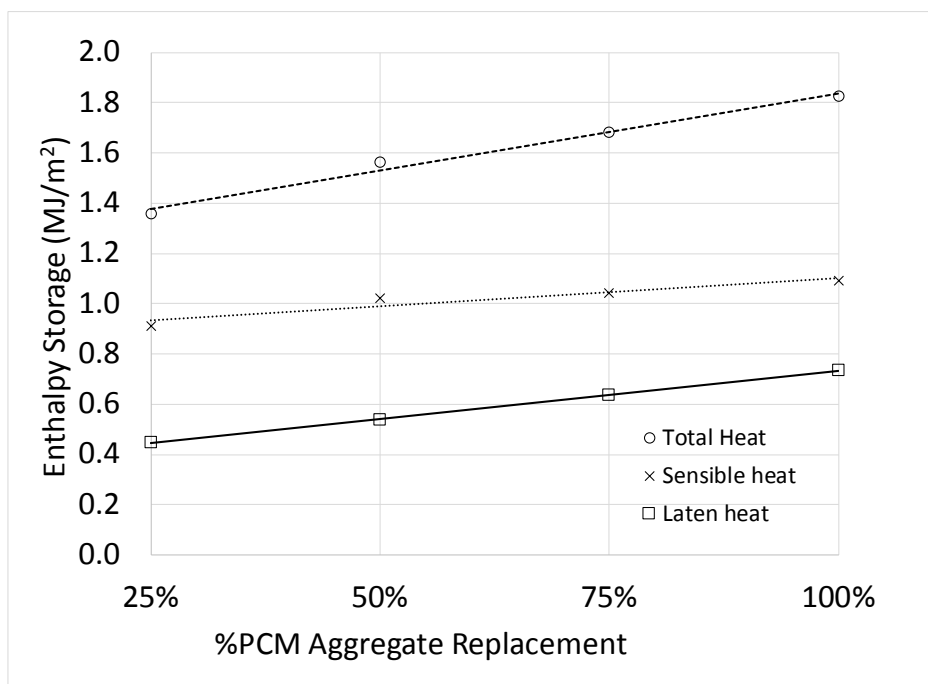
$$404 \quad h_l = 0.39(A_{PCM}) + 0.35 \quad (7)$$

405 where A_{PCM} is the percentage replacement of PCM aggregate over the conventional
 406 lightweight aggregate.

407 Table 6 Total heat, Specific heat and Latent heat

	Unit	75L25P	50L50P	25L75P	0L100P
Total Heat/sq.m	MJ/m ²	1.36	1.56	1.68	1.83
Specific heat of solid PCM	(MJ/m ²)/°C	0.136	0.139	0.142	0.150
Specific heat of melted PCM	(MJ/m ²)/°C	0.168	0.202	0.206	0.214
Sensible heat/sq.m	MJ/m ²	0.910	1.024	1.043	1.092
Latent heat/sq.m	MJ/m ²	0.447	0.539	0.637	0.735
Latent heat capacity	J/kg	4,847	5,828	6,781	7,722

408



409

410 Fig. 11 Relationships between PCM Aggregate Replacement Percentage and Heat Storage

411

412 **4. Conclusions**

413 In this study, the thermal properties essential for lightweight concrete mixed with aggregates
 414 impregnated with PCM (polyethylene glycol 1450) were determined. The rate of replacement
 415 of conventional porous aggregates with PCM impregnated aggregates ranged from 25 % to
 416 100% (equivalent to 2.1 to 7.8% by weight of concrete).

417 Thermal conductivity tested under solid state PCM (TC_s or TC_{25}) was found to increase with
 418 the PCM aggregate content from 0.448 W/m°C to 0.841 W/m°C due to the increase in solid
 419 content where solid PCM is replacing voids inside the aggregates. Under liquid state PCM, the
 420 TC_M or TC_{55} was found to decrease with increasing PCM aggregate content from 0.647 W/m°C
 421 to 0.456 W/m°C due to the effect of energy storage during the PCM's phase changing process.

422 For latent heat and sensible heat storage, both were found to increase with the PCM
423 aggregate content to varying degrees. A 20% increase is observed in the sensible heat, mainly
424 due to the increasing specific heat (especially in the C_{pM}) with PCM aggregate content. The
425 specific heat is relatively constant for all types of concrete when tested under PCM solid state.
426 However, a large increase in specific heat is observed when concretes are tested under PCM
427 liquid state.

428 Latent heat is found to increase significantly (by 64%) when the PCM aggregates replacement
429 rate rises from 25 % to 100%. The effect of energy storage during phase changing of PCM
430 plays an important role on increasing latent heat storage.

431 The improvement in both mechanical and the latent heat properties with the increasing PCM
432 content indicates the possibility of incorporating high contents of PCM into concrete without
433 compromising other required properties. In this study, a maximum latent heat of 7,722 J/kg
434 and compressive strength of 25.4 MPa was found in lightweight concrete with a PCM content
435 of 7.8% by weight of concrete.

436 **Acknowledgements**

437 This project is funded by Thailand Research Fund – Research and Researchers for Industries
438 (TRF-RRI) under contract no. MSD61I0019 (Pattra Uthaichotirat) and TRF Distinguished
439 Research Professor grant no. DPG6180002 (Prof. Prinya Chindapasirt). The authors declare
440 that they have no conflict of interest. The authors would like to thank also to Siam Research
441 and Innovation Co., Ltd.

442 **References**

- 443 [1] Rao, V. V., Parameshwaran, R., & Ram, V. V., PCM-mortar based construction materials
444 for energy efficient buildings: A review on research trends. *Energy and Buildings*, 158
445 (2018), 95-122.
- 446 [2] Diana Üрге-Vorsatz, Luisa F. Cabeza, Susana Serrano, Camila Barreneche, Ksenia
447 Petrichenko, Heating and cooling energy trends and drivers in buildings, *Renewable and*
448 *Sustainable Energy Reviews*, 41 (2015): 85-98.
- 449 [3] Energy Policy and Planning Office, Ministry of Energy, *Energy Statistic of Thailand 2018*,
450 2018.
- 451 [4] Sharma, SK., Zero energy building envelope components: a review, *Int. J. Eng Res Appl.*,
452 3, no.2(2013): 662–675.
- 453 [5] Abhat A., Low temperature latent heat thermal energy storage, *Heat storage materials*,
454 *Solar Energy*, 30 (1983): 313–332.
- 455 [6] Lorsch H.G., Kauffman K.W., Denton J.C., Thermal energy storage for heating and air
456 conditioning, future energy production system, *Heat Mass Transfer Proc.*, 1 (1976): 69–
457 85.
- 458 [7] Abhat A, et al., Development of a modular heat exchanger with an integrated latent
459 heat storage, Report no. BMFT FBT 81-050, Germany Ministry of Science and
460 Technology Bonn, 1981.
- 461 [8] Hale D.V., Hoover M.J., O'Neill M.J., *Phase change materials handbook*. Alabama
462 Marshal Space Flight Center, 1971.
- 463 [9] Telkes M., Solar house heating—a problem of heat storage, *J. Heat Ventilating*, 44
464 (1947): 68–75.
- 465 [10] Oliver A., Thermal characterization of gypsum boards with PCM included: Thermal
466 energy storage in buildings through latent heat, *Energy and Buildings*, 48 (2012): 1-7.

- 467 [11] Silva T., Vicente R., Rodrigues F., Samagaio A., Cardoso C., Performance of a window
468 shutter with phase change material under summer Mediterranean climate conditions.
469 Applied Thermal Engineering 84 (2015): 246-256.
- 470 [12] Cunha S., Lima M., Aguiar J., Influence of adding phase change materials on the
471 physical and mechanical properties of cement mortars, Construction and Building
472 Materials, 127 (2016): 1-10.
- 473 [13] Sukontasukkul P., Sutthiphasilp T., Chalodhorn W. and Chindaprasirt P., Improving
474 thermal properties of exterior plastering mortars with phase change materials with
475 different melting temperatures: paraffin and polyethylene glycol, Advances in Building
476 Energy Research (2018), DOI: 10.1080/17512549.2018.1488614
- 477 [14] Boh B., Sumiga B., Microencapsulation technology and its applications in building
478 construction materials, RMZ—Materials and Geoenvironment, 55, no.3 (2008): 329–
479 44.
- 480 [15] Hawlader M.N.A., Uddin M.S., Khin M.M., Microencapsulated PCM thermal energy
481 storage system, Applied Energy, 74 (2003): 195–202.
- 482 [16] Ling T-C, Poon C-S, Use of phase change materials for thermal energy storage in
483 concrete: An overview, Construction and Building Materials, 46 (2013): 55-62.
- 484 [17] Cao V.H., Pilehvar S., Salas-Bringas C., Szczotok A.M., Rodriguez J.F., Carmona M., Nodar
485 Al-Manasir, Kjøniksen A., Microencapsulated phase change materials for enhancing the
486 thermal performance of Portland cement concrete and geopolymer concrete for
487 passive building applications, Energy Conversion and Management, 133 (2017): 56-66.
- 488 [18] Sakulich, A. R., & Bentz, D. P., Incorporation of phase change materials in cementitious
489 systems via fine lightweight aggregate, Construction and Building Materials, 35 (2012),
490 483-490.

- 491 [19] Sukontasukkul, P., Intawong, E., Preemanoch, P. Chindaprasirt, P., Use of paraffin
492 impregnated lightweight aggregates to improve thermal properties of concrete panels,
493 Materials and Structures 49 (2016): 1793.
- 494 [20] Amitha Jayalath, Rackel San Nicolas, Massoud Sofi, Robert Shanks, Tuan Ngo, Lu Aye,
495 Priyan Mendis, Properties of cementitious mortar and concrete containing micro-
496 encapsulated phase change materials, Construction and Building Materials, 120 (2016):
497 408-417. <https://doi.org/10.1016/j.conbuildmat.2016.05.116>.
- 498 [21] Ramakrishnan, S., Sanjayan, J., Wang, X., Alam, M., & Wilson, J. (2015). A novel
499 paraffin/expanded perlite composite phase change material for prevention of PCM
500 leakage in cementitious composites. Applied Energy, 157, 85-94.
- 501